Plasmonic-Coupling-Based Sensing by the Assembly and Disassembly of Dipycolylamine-Tagged Gold Nanoparticles Induced by Complexing with Cations and Anions

ARTICLE *in* SMALL · MAY 2012

Impact Factor: 8.37 · DOI: 10.1002/smll.201102335 · Source: PubMed

6 AUTHORS, INCLUDING:

Dongxiang Li
Qingdao University of Science and Technol…
35 PUBLICATIONS **1,014** CITATIONS
SEE PROFILE

Yoon Hee Jang
Korea Institute of Science and Technology
36 PUBLICATIONS **510** CITATIONS
SEE PROFILE

Dong Ha Kim
Ewha Womans University
136 PUBLICATIONS **3,157** CITATIONS
SEE PROFILE

Plasmonic-Coupling-Based Sensing by the Assembly and Disassembly of Dipycolylamine-Tagged Gold Nanoparticles Induced by Complexing with Cations and Anions

Dong Xiang Li, Jun Feng Zhang, Yoon Hee Jang, Yu Jin Jang, Dong Ha Kim, and Jong Seung Kim**

A *surface-plasmon-coupling-mediated sensor system is developed based on Au nanoparticles tagged with a coordinative dipycolylamine and lipoyl-anchored naphthalimide derivative (AuNP@DPA). The AuNPs with tailored ligands exhibit distinct sensing activity via sequential assembly into nanoparticle aggregates induced by metal ion complexing, and disassembly in the presence of pyrophosphate (PPi) anions, which is accompanied by a swift, reversible color change due to a surface plasmon resonance coupling effect. It is found that divalent metal ions are more effective than mono- or tri-valent ions in the aggregate formation process, Mn^{2+}-induced aggregates are more sensitive to the capture of PPi anions than other AuNP aggregates, and the disassembly upon anion complexation exhibits a highly selective response. The AuNP@DPA-based molecular recognition system also demonstrates a viable performance for the detection of total selective metal ions present in different types of water analytes.*

Prof. D. X. Li,[+] Y. H. Jang, Y. J. Jang, Prof. D. H. Kim
Department of Chemistry and Nano Science
Ewha Womans University
52, Ewhayeodae-gil,
Seodaemun-gu, Seoul 120-750, Korea
E-mail: dhkim@ewha.ac.kr
Prof. D. X. Li[+]
College of Chemistry and Molecular Engineering
Qingdao University of Science and Technology
Qingdao, 266042, PR China
Prof. J. F. Zhang,[+] Prof. J. S. Kim
Department of Chemistry
Korea University
Seoul 136-701, Korea
E-mail: jongskim@korea.ac.kr
Prof. J. F. Zhang [+]
College of Chemistry and Chemical Engineering
Yunnan Normal University
Kunming, 650092, PR China
[+] These authors contributed equally to this work.

DOI: 10.1002/smll.201102335

1. Introduction

The controlled assembly of gold nanoparticles (AuNPs) has attracted much attention due to their unique localized surface plasmon resonances (LSPRs).[1–5] Ordered assemblies of AuNPs result in interparticle surface plasmon resonance (SPR) coupling due to reduced average interparticle spacing; they also exhibit color changes[6,7] and red-shifted characteristic LSPR bands in their UV-vis extinction spectra.[8–10] Such SPR coupling-based color changes of noble metal nanoparticles have been considered versatile tools for developing sensitive and selective molecular recognition systems, with colorimetric sensing investigated for application in biological assays[11–16] and metal ion detection.[17–20]

Mechanisms for the formation of Au nanoaggregates involve "crosslinking aggregation" or "non-crosslinking aggregation" between neighboring nanoparticles; the former was applied in the majority of previous works, in which the detection targets usually act as linkers for surface-functionalized AuNPs. Specific DNA-based recognition has been explored for colorimetric sensing[21,22] using thymine (T-base)-rich

small NANO MICRO

DNA for mercury(II) probing[23–25] and uracil (C-base)-rich DNA for silver(I) sensing.[26] Non-crosslinking aggregation can be mediated via specific interactions, including coordinative interactions for the detection of mercury(II) ions,[27–29] electrostatic interactions via the carboxyl periphery for lead(II) detection,[30,31] or the dopamine/cysteine shell for copper ions,[32–34] H-bonding,[35,36] double molecular recognition,[37] and supramolecular interactions.[15,38] To demonstrate target recognition, the removal of stabilizer ligands from nanoparticle surfaces has been reported to cause AuNPs to aggregate[39] and the presence of Hg(II)/Ag(I) ions can prevent such aggregation.[40] The oxidation of thiol-terminated AuNPs by dichromate anions also resulted in their aggregation, allowing detection of chromium(VI) ions.[41] Although coordinating interactions have been employed in AuNP-based colorimetric assays, the use of strongly coordinating compounds with three nitrogen ligands for metal ion detection has not been previously reported.

A selective fluorescent chemosensor has been developed for the detection of pyrophosphate (PPi) anions. It shows large differences of fluorescence based on interactions of Cu(II) ions and coordinative dipycolylamine (DPA)-anchored naphthalimide compounds in a mesoporous silica-immobilized naphthalimide–DPA–copper(II) complex.[42] However, designing the tailored fluorescent molecules and their multiple-step synthesis were laborious. This work reports the integration of similar recognition elements on the surfaces of AuNPs, with DPA-tagged AuNPs demonstrating a plasmonic-coupling-based highly selective sensing of PPi anions (**Figure 1**a).

2. Results and Discussion

DPA and lipoyl anchored naphthalimide, compound **1** (Figure 1), was prepared from bis(2-pyridylmethyl) amine (DPA), 4-bromo-1,8-naphthalic anhydride and lipoic acid via

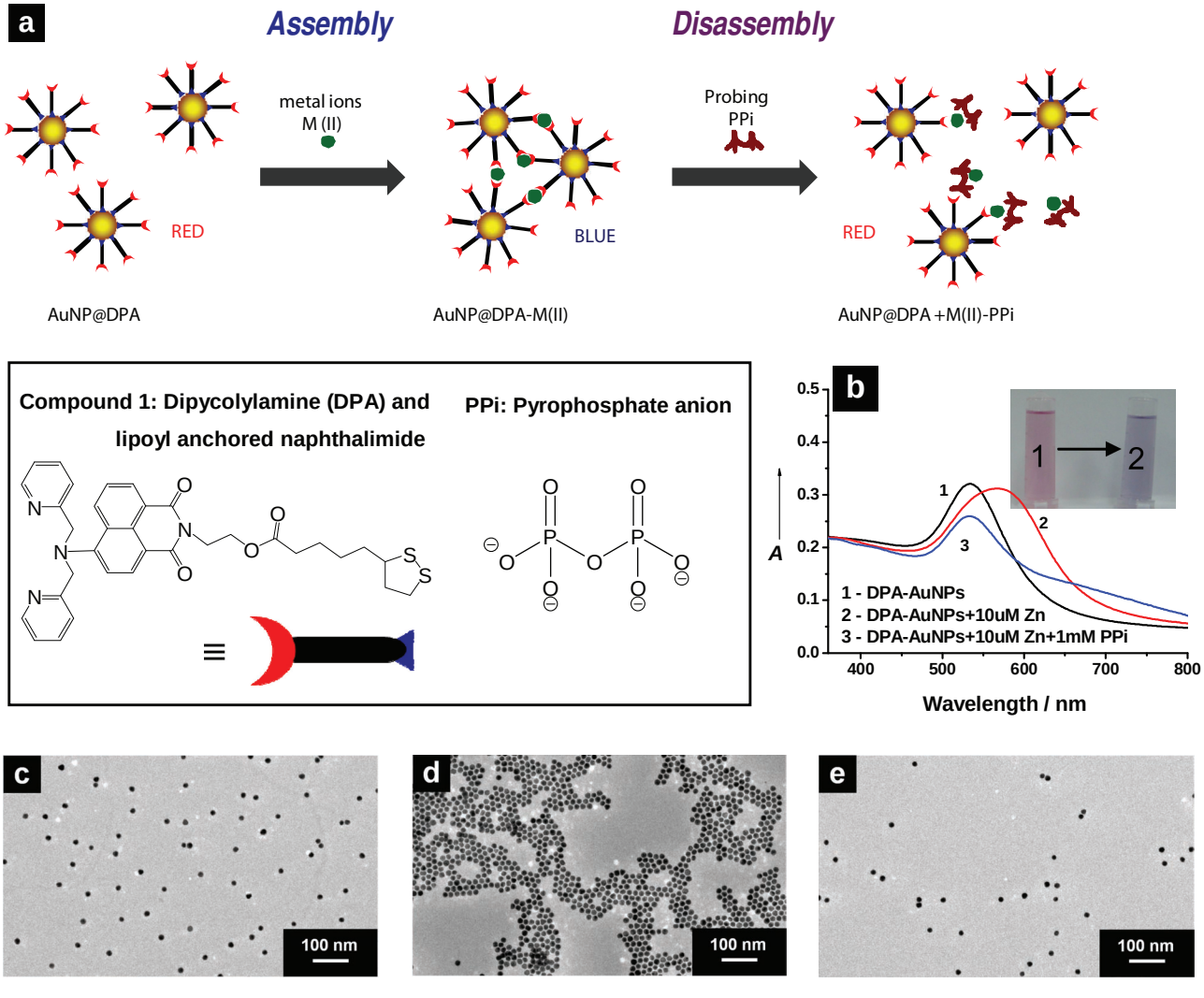

Figure 1. a) The sequential assembly of DPA-tagged AuNPs (AuNP@DPA) through coordinative connection by metal ions and the selectively responsive disassembly in the probing of pyrophosphate (PPi) anions. b) UV-vis spectra of DPA-tagged AuNPs (line 1), Zn^{2+}-induced nanoparticle aggregates (line 2) and PPi-induced disassembly of nanoparticle aggregates (line 3) in chloroform. c–e) TEM images, in chloroform, of: DPA-tagged AuNPs (c), Zn^{2+}-induced nanoparticle aggregates (d), and, PPi-induced disassembly of nanoparticle aggregates (e).

a modification of a previously reported method.[42] Then, **1** was directly immobilized onto the surfaces of AuNPs to fabricate DPA-tagged AuNPs (AuNP@DPA), which were subsequently assembled into aggregates induced by complexing with various metal cations. This resulted in a swift color change from red to blue, due to enhanced SPR coupling. The resulting aggregates could then disassemble in the presence of PPi anions, with a concurrent rapid return to appearing red in color. Such sequential assembly and disassembly could be used as a colorimetric assay for the selective recognition of PPi anions.

DPA-tagged AuNPs (AuNP@DPA) were fabricated by dropping citrate-capped Au colloids into a solution of **1** to induce ligand exchange between the citrate and dithiol groups, leading to the formation of Au-S covalent bonds on the nanoparticles' surfaces.[1] The fluorescence spectrum of a mixture of colloidal AuNPs and **1** was gradually quenched by fluorescence resonance energy transfer from naphthalimide to the AuNPs (Figure S1 in the Supporting Information), implying that **1** was successfully bound to the AuNPs' surfaces. Note that **1** with 1,2-dithiol terminal groups would be more strongly anchored to the Au surfaces due to the formation of two Au–S bonds. AuNP@DPA could not be dispersed in water, alcohol, THF, or acetonitrile, but were well-dispersed in chloroform, reflecting their hydrophobicity. The SPR band of AuNP@DPA suspended in chloroform (Figure 1b, line 1) was centered at approximately 533 nm, showing typical behaviour for well-dispersed colloidal nanoparticles. The addition of 10 μM Zn^{2+} resulted in the suspension rapidly turning blue (Figure 1b, inset); the characteristic SPR band shifted to approximately 567 nm within 1 min (Figure 1b, line 2). This was attributed to enhanced plasmonic coupling, i.e., the formation of AuNP aggregates,[6] driven by the Zn^{2+} crosslinking neighboring AuNP@DPA nanoparticles through complexing between the coordinative DPA moieties and unoccupied orbitals of Zn^{2+}.[42] The addition of PPi solution to this aggregate suspension effected its swift return to red and the blue-shifting of its SPR band to the original approximate 533 nm (Figure 1b, line 3). In fact, the Zn^{2+}-induced AuNP aggregates are formed via the coordination between Zn^{2+} and DPA groups because one Zn^{2+} ion can connect two DPA groups immobilized on different AuNPs. After PPi addition, the disassembly of these AuNP aggregates is induced due to the competitive complexation of PPi with Zn^{2+} based on their strong interaction. Thus, such a competitive complexation between PPi with Zn^{2+} can destroy the coordination between Zn^{2+} and DPA groups, i.e., the role of Zn^{2+} in the connection of two DPA groups on different AuNPs disappears. Then, the interparticle crosslinking is broken and the two AuNPs are isolated.[43,44] Note that metal ions can be released from DPA at high concentrations of PPi.[42]

The sequential assembly and disassembly was verified by TEM. AuNP@DPA were well-dispersed in chloroform with an average size of 13.5 nm (Figure 1c and Figure S2 in the Supporting Information). The addition of 10 μM Zn^{2+} resulted in well-defined ordered assemblies of AuNPs (Figure 1d) due to interparticle crosslinking. The typical interparticle distance of the AuNPs was ca. 2.0 nm, twice the size of the ligand of **1,** as theoretically expected. The AuNP@DPA nanoparticles

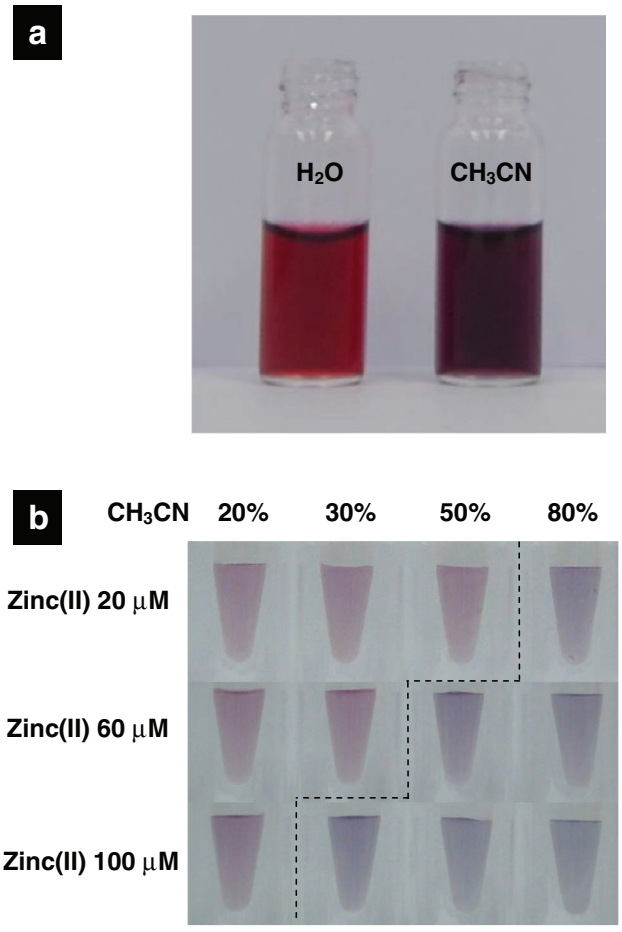

Figure 2. Optical photos of: a) hydrophilic DPA-tagged AuNPs dispersed in water (left) and in acetonitrile (right), and, b) the color changes of hydrophilic DPA-tagged AuNPs in water/acetonitrile mixture with labeled acetonitrile content after the addition of different amount of Zn^{2+} ions.

became mono-dispersed upon the subsequent addition of PPi (Figure 1e).

Although chloroform was used in the demonstration of the overall concept and the experimental strategy proposed in Figure 1, it is very volatile, which may limit its applicability in sensing. To overcome this, coordinative AuNP@DPA were developed that could be aqueously dispersed. Concretely, poly(ethylene glycol) (PEG)–thiol and 11-mercaptoundecanoic acid (MUA) were used to modify AuNPs together with **1** to render hydrophilic moieties and electrostatic stabilization to the surface of AuNPs. The feed ratio of DPA/PEG–thiol/MUA was controlled at approximately 1:1:10, and the obtained hydrophilic AuNP@DPA nanoparticles displayed a good dispersity in water (red color) and a relatively low dispersity in acetonitrile (purple color), as shown in **Figure 2**a. However, we found that the aqueous suspension of hydrophilic AuNP@DPA did not show distinctly responsive behaviour to Zn^{2+} ions, which might be due to the low coordinative efficiency of DPA moieties to metal ions in water. To our knowledge, changing solvent polarity can adjust the complexation function, so it is conjectured that addition of immiscible solvent CH_3CN into water may be helpful to enhance the sensitivity to metal ions. To determine the

small NANO MICRO

influence of CH_3CN content in solvent mixtures, a series of H_2O/CH_3CN mixtures containing 20%, 30%, 50%, and 80% CH_3CN, respectively, were used to disperse the hydrophilic AuNP@DPA and then their response was investigated by adding different amounts of Zn^{2+} ions (Figure 2b). It was found that adding 20 μM Zn^{2+} ions can induce aggregate formation only in the solvent mixture with 80% CH_3CN, adding 60 μM Zn^{2+} ions can change the color of the two systems containing 50% and 80% CH_3CN, and adding 100 μM Zn^{2+} ions can make the three systems containing 30%, 50% and 80% CH_3CN change. This indicates that more acetonitrile content in the solvent mixture is advantageous to attain a higher sensitivity of AuNP@DPA suspensions to Zn^{2+} ions. Further experiments were performed to investigate the nanoparticles' selectivity in a mixed H_2O/CH_3CN (20:80 v/v) solvent system, because a suitable water content allowed the effective dissolution of the metal ions.

The plasmonic-coupling-induced color changes were investigated by adding different amounts of Zn^{2+} and Mn^{2+} to hydrophilic AuNP@DPA suspensions. The results obtained by adding Zn^{2+} and Mn^{2+} ions are displayed in **Figure 3**a and b, respectively. Adding 2.0 μM of Zn^{2+} and Mn^{2+} ions did not cause a color change, although relatively small SPR shifts of 5 and 20 nm, respectively, were found. Adding 5.0 μM metal ions led to a purple color after 2 min and an SPR red shift by approximately 60 nm after 3 h, while adding 10 μM of Zn^{2+} or Mn^{2+} ions brought about rapid color changes from red to blue within 1 min. It was found that the concentration effect was similar for the two metal ions and the rapid response was observed at approximately 10 μM concentration of metal ions, which might represent an effective detection limit for practical use.

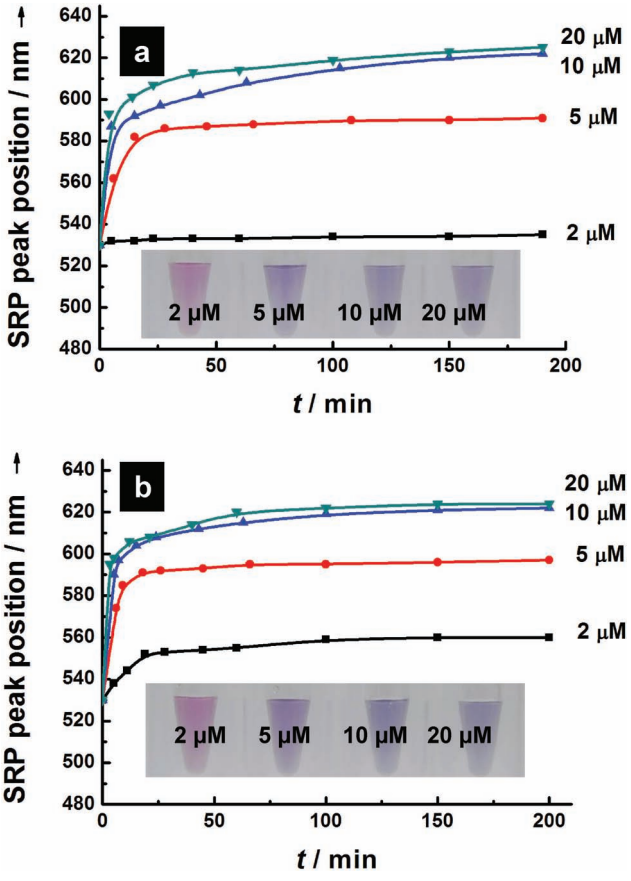

Figure 3. Concentration effect of Zn^{2+} (a) and Mn^{2+} (b) ions on the assembly of hydrophilic DPA-tagged AuNPs in a mixed solvent of H_2O and CH_3CN (20:80). The inserted photos show the sample color change taken at 2 min after metal ion addition.

The detection of different metal ions, i.e., the ability to form AuNP aggregates, was tested for Ni^{2+}, Cd^{2+}, Cu^{2+}, Fe^{3+}, Zn^{2+}, Ag^{+}, Al^{3+}, Co^{2+}, Hg^{2+}, Mn^{2+}, Pb^{2+}, Fe^{2+}, Ca^{2+}, Mg^{2+}, Na^{+}, K^{+}, Li^{+}, Sr^{2+}, Sn^{2+}, and Pd^{2+}. Color changes and SPR band peak positions upon the addition of 20 μM of each metal ion and the subsequent addition of 40 μM PPi were measured (**Figure 4**). Only some of the metal ions effected color changes. All the divalent metal ions induced color changes, with Ni^{2+}, Cd^{2+}, Zn^{2+}, Co^{2+}, Mn^{2+}, Pb^{2+}, Fe^{2+}, Ca^{2+}, Mg^{2+}, and Sr^{2+} effecting rapid color changes and Cu^{2+}, Sn^{2+}, Hg^{2+}, and Pd^{2+} acting more slowly. Trivalent Fe^{3+} and Al^{3+} and monovalent Na^{+}, K^{+}, Li^{+}, and Ag^{+} did not induce color changes. Therefore, the valence state of the metal ions appeared to be critical to the formation of aggregates, as it directly affected the charges on the nanoparticles' surfaces upon the adsorption of the metal ions. Non-transition metal ions Ca^{2+}, Mg^{2+}, Sr^{2+}, Sn^{2+}, and Pd^{2+} could also induce nanoparticle assembly, indicating that it was due not only to coordinative interactions between the DPA moieties and the metal ions, but also to electrostatic interactions between partially ionized carboxyl groups of MUA and the metal ions.[30,31] The trivalent ions' higher charges likely induced strong electrostatic repulsions between the nanoparticles that prevented their aggregation.

The subsequent addition of 40 μM PPi to the assembled AuNPs led to partial or complete recovery of their original red color with concurrent blue-shifting of their characteristic SPR bands. The aggregates induced by Ni^{2+}, Cd^{2+}, Cu^{2+}, Zn^{2+}, Co^{2+}, Pb^{2+}, Fe^{2+}, Ca^{2+}, Mg^{2+}, Sr^{2+}, Sn^{2+}, and Pd^{2+} showed partial color recovery with some SPR peak shift. The Mn^{2+}-induced aggregates displayed rapid color recovery and blue shifting of its SPR band by approximately 2 nm compared with the initial well-dispersed suspension. The assemblies induced by Ag^{+}, Al^{3+}, and Hg^{2+} were further aggregated upon the addition of PPi, while those induced by Li^{+}, Na^{+}, and K^{+} did not show any response to PPi.

The rapid responses of the Mn^{2+}-induced aggregates to PPi suggested their suitability for testing the selectivity of their disassembly driven by various other anions: citrate, ascorbate, oxalate, acetate, NO_3^-, SCN^-, CN^-, $H_2PO_4^-$, HPO_4^-, PO_4^-, ClO_4^-, HSO_4^-, SO_4^-, F^-, Cl^-, Br^-, and I^-. These anions were gradually added at 10 to 800 μM to the Mn^{2+}-induced aggregates and the color changes were measured (**Figure 5**). The results show that addition of 10 μM PPi could induce disassembly of the Mn^{2+}-induced aggregates, implying selectivity to tetravalent anions. 80 μM divalent oxalate and 500 μM trivalent citrate anions resulted in similar disassembly (Figure 5, red circles). These multivalent anions possess coordinative carbonyl moieties and different degrees of electric charge, allowing them to coordinate to the DPA moieties in competition with Mn^{2+}, leading to the aggregates' disassembly. Highly charged anions could make the nanoparticles' surfaces negatively charged, causing electrostatic repulsions between

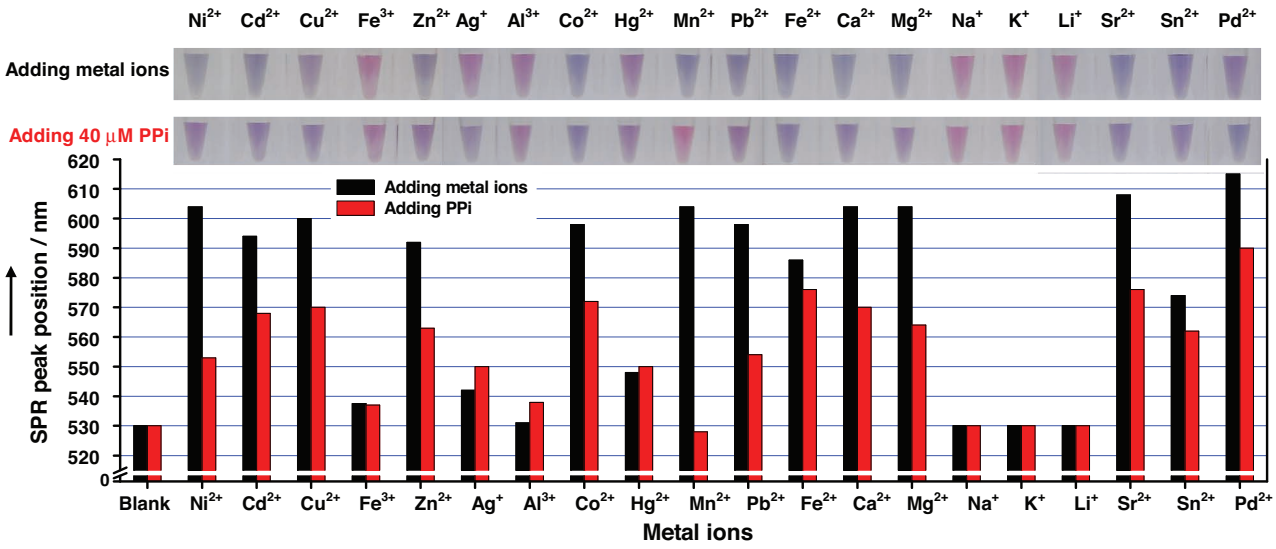

Figure 4. Changes of color and SPR peak position of hydrophilic AuNP@DPA suspensions in H_2O/CH_3CN (20:80) upon the addition of 20 μM metal ions (upper photo array, black columns) and the subsequent addition of 40 μM PPi (lower photo array, red columns).

them and accelerating the aggregates' disassembly. $H_2PO_4^-$, HPO_4^{2-}, and PO_4^{3-} (Figure 5, yellow circles) did not greatly induce aggregates' disassembly because HPO_4^{2-} and PO_4^{3-} are multiple anions and $H_2PO_4^-$ can be ionized to multiple anions. The phosphorus oxygen bonds could also coordinate to metal ions. Monovalent and non-coordinative anions, acetate, NO_3^-, SCN^-, CN^-, ClO_4^-, HSO_4^-, SO_4^-, F^-, Cl^-, Br^-, and I^- showed no ability to break the aggregates due to their low charge. Un-ionizable ascobate showed a similar lack of activity. Sensitive and selective Mn^{2+}-induced AuNP aggregates demonstrated versatile functionality for the recognition of traces of analytes. As a product of cellular ATP hydrolysis, PPi is an important bioenergetic and metabolic target. Its detection using these tagged AuNPs may aid real-time DNA sequencing, bioassays,[43,44] and cancer diagnosis.[45,46] The above results show that 10 μM PPi was the minimum level to effect recovery of the red color and that 20 μM led to the complete disassembly of the Mn^{2+}-induced AuNP@

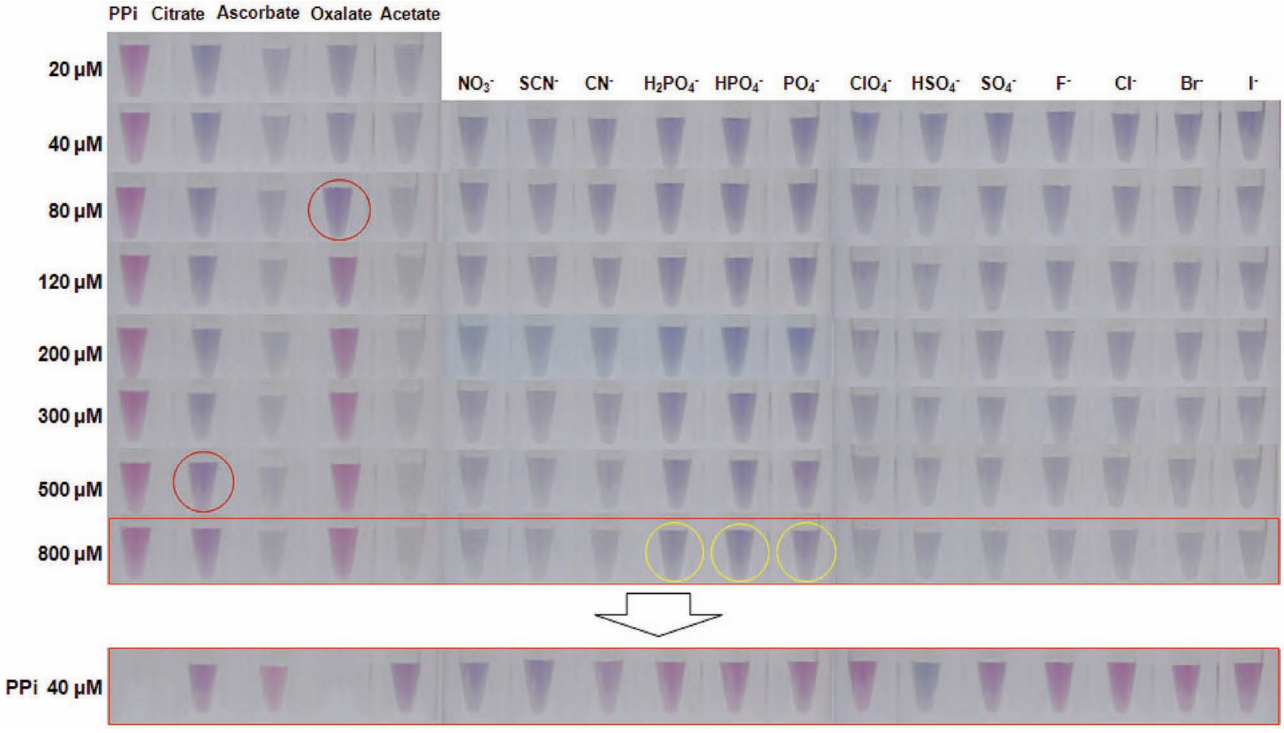

Figure 5. Color changes of blue Mn^{2+}-induced nanoaggregates upon the addition of various anions (top) at increasing concentrations (left). Red circles show critical anion concentrations for red color recovery. Yellow circles show weak color changes. Samples with 800 μM anions (upper red rectangle, except PPi and oxalate) had 40 μM PPi added (lower red rectangle).

NANO MICRO small

DPA aggregates. At such levels, no other anions affected the detection of PPi, with only higher concentrations of oxalate and citrate, 8 and 50 times, respectively, inducing similar disassembly. Note that the interactions of phosphate ions could be ignored because only a concentration 80 times that of PPi could give a weak signal and such high concentrations of phosphate ions would cause further aggregation due to the increased ionic strength. To assess the effects of PPi in the presence of other anions, it was added at 40 μM to samples containing 800 μM of other anions (except oxalate) and color changes were monitored (Figure 5, red rectangles). Red color recovery of the Mn^{2+}-induced aggregates was observed upon the addition of 40 μM PPi to suspensions containing 800 μM ascorbate, $H_2PO_4^-$, HPO_4^{2-}, PO_4^{3-}, ClO_4^-, SO_4^{2-}, F^-, Cl^-, Br^-, or I^-, indicating that high concentrations of these anions did not interfere with the aggregates' recognition of PPi. However, 800 μM NO_3^-, SCN^-, HSO_4^-, and CN^- did affect PPi recognition. Therefore, the recognition of PPi by Mn^{2+}-induced AuNP aggregates is highly selective, suggesting their potential applicability as probes for PPi detection.

All the tested divalent metal ions could act as linkers to couple the AuNP@DPA suspensions. Such suspensions could also be used to estimate the total concentration of all the sensitive metal ions present in mixed analytes (**Figure 6**). Five different types of water, including ground rain (clear-flowing rain water on ground), pipe water (tap water), drinking water (from drink machine), primary water (once-distilled water), and ultrapure water (resistivity ≥18.2 MΩ•cm), were used to analyze the total content of sensitive metal ions. The color and SPR peak changes showed that 1.0 μL of any water cannot induce nanoparticle assembly, while 2.0 μL ground rain, 3.3 μL pipe water and 5 μL drinking water caused the color change, concurrent with an SPR peak shift from 530 to 570–580 nm. However, primary water and ultrapure water did not bring about any noticeable color change. If any metal ions are assumed to have a driving force similar to Zn^{2+}/Mn^{2+} ions, the samples with critical color change may contain a total concentration of approximately 10 μM selective metal ions, judging from the Zn^{2+}/Mn^{2+}-based results. Thus, the total concentration of sensitive metal ions in ground rain, pipe water and drink water can be deduced to be about 2.5, 1.5, and 1.0 mM, respectively. In addition to these applications, other strategies could also be employed with the AuNP@DPA-based recognition system to enhance its selectivity and sensitivity.[23] For example, using buffer solution can adjust the ionic strength and/or pH for improved sensitivity[20] and the addition of specific ligands to analytes can induce the preferential formation of coordination complexes, thus masking the effects of interfering ions.[28,47]

3. Conclusion

In summary, a coordinative DPA and lipoyl anchored naphthalimide derivative was synthesized to fabricate DPA-tagged AuNPs. The addition of metal ions could induce the particles to assemble into aggregates, changing their color due to surface plasmon resonance coupling effects. Divalent metal ions were found to be more effective than mono- or trivalent ions because of a combination of coordinative forces

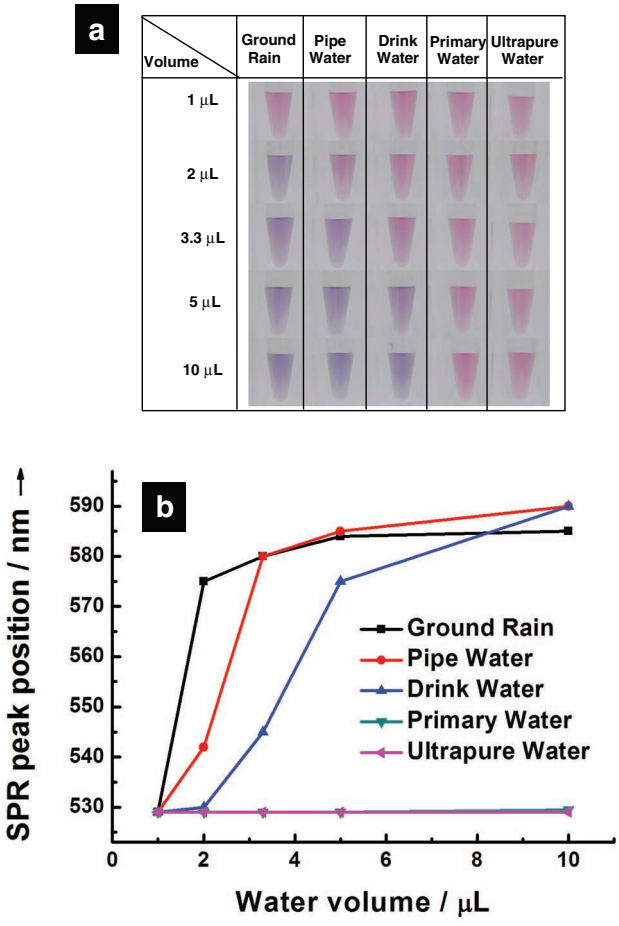

Figure 6. a) Color changes, and, b) SPR peak changes of hydrophilic DPA-tagged AuNPs in water/acetonitrile (20:80) upon the addition of different volume of five types of waters.

and electrostatic interactions between the nanoparticles and the metal ions. AuNP@DPA-based molecular recognition was used for the selective detection of certain aqueous metal ions. The resulting metal ion-induced aggregates of DPA-tagged AuNPs were rapidly disassembled upon the addition of PPi anions, with those originally formed by Mn^{2+} showing the most sensitive responses to PPi. The assembly and disassembly of the AuNP@DPA aggregates was driven by their specific affinity towards target analytes mediated by plasmonic coupling phenomena and may provide a basis for the development of highly selective and sensitive recognition systems for environmental remediation and biomedical diagnosis.

4. Experimental Section

Synthesis and Characterization of Compound **1**: Dipycolylamine (DPA) and lipoyl anchored naphthalimide, **1**, was synthesized via a three-step reaction (Figure S3 in the Supporting Information). First, compound **3** was synthesized as reported elsewhere.[42] Compound **3** (0.3 g, 0.76 mmol) and 2-aminoethanol (0.1 g, 1.64 mmol) in EtOH (50 mL) was refluxed for 24 h, evaporated, redissolved in CH_2Cl_2 (100 mL), washed with water (3 × 50 mL), dried over anhydrous Na_2SO_4, and filtered. The solution was evaporated to yield crude product, which was purified by silica gel column chromatography

(**2**: 0.26 g, 79% yield, Figure S4). A solution of **2** (200 mg, 0.46 mmol), (±)-α-lipoic acid (100 mg, 0.49 mmol), *N*-(3-dimethylaminopropyl)-*N'*-ethylcarbodiimide hydrochloride (EDCI) (100 mg, 0.52 mmol) and 4-*N*,*N*-dimethylaminopyidine (DMAP) (60 mg, 0.49 mmol) in DMF (10 mL) was stirred at room temperature for 12 h, added to H_2O (50 mL), extracted with ethyl acetate (3 × 50 mL), dried over anhydrous Na_2SO_4, and filtered. The crude product was obtained by rotary evaporation and purified by column chromatography (**1**: 0.21 g, 73% yield, Figure S5).

Fabrication of DPA-Tagged AuNPs (AuNP@DPA): *Ca.* 0.8 nM AuNPs were prepared by conventional citrate-reduction. First, an equal volume of colloidal gold was dropped into a solution of **1** (0.5 mM in THF) and stirred overnight, then the resultant AuNP@DPA nanoparticles were centrifuged and washed with THF/chloroform. They were dispersed in chloroform as hydrophobic samples. Gold colloid was then dropped into an equal volume of 0.05 mM **1**, 0.05 mM *O*-(2-mercaptoethyl)-*O'*-methyl-hexa(ethylene glycol) (PEG-thiol) and 0.5 mM 11-mercaptoundecanoic acid (MUA) in THF, resulting in hydrophilic AuNP@DPA samples, which were then dispersed in water or acetonitrile for subsequent use.

Assembly and Disassembly Experiments: The DPA-tagged AuNPs (AuNP@DPA) were adjusted to ca. 0.4 nM for the assembly and disassembly tests. 10 mM stock solutions of various metal ions and anions were used directly or diluted. The solvent was water and acetonitrile at a volume ratio of 20:80.

Supporting Information

Supporting Information is available from the Wiley Online Library or from the author.

Acknowledgements

This work was supported by grants from the International Research & Development Program (2010-00134), the Mid-Career Researcher Program (20110029409), the SRC Program (20110001334) and a CRI project (2011-0000420) through the National Research Foundation (NRF) of Korea, funded by the Korean Government, and was supported by the Ewha Global Top5 Grant 2011 of Ewha Womans University. J.F.Z. acknowledges the Program for Changjiang Scholars and Innovative Research Team in University (PCSIRT) and the Foundation of the Department of Science and Technology of Yunnan Province of China (2011FB047). D.X.L. was supported by an RP-Grant 2011 from Ewha Womans University.

[1] M. C. Daniel, D. Astruc, *Chem. Rev.* **2004**, *104*, 293.
[2] F. Westerlund, T. Bjornholm, *Curr Opin. Colloid Interface Sci.* **2009**, *14*, 126.
[3] X. H. Zhou, J. R. Li, C. Y. Liu, L. Jiang, *Sci. China, Ser. B: Chem.* **2002**, *45*, 358.
[4] C. H. Lalander, Y. Zheng, S. Dhuey, S. Cabrini, U. Bach, *ACS Nano* **2010**, *4*, 6153.
[5] D. X. Li, J. Y. Lee, D. H. Kim, *J. Colloid Interface Sci.* **2011**, *354*, *585*.
[6] S. K. Ghosh, T. Pal, *Chem. Rev.* **2007**, *107*, 4797.
[7] N. J. Halas, S. Lal, W. S. Chang, S. Link, P. Nordlander, *Chem. Rev.* **2011**, *111*, 3913.
[8] X. G. Han, J. Goebl, Z. D. Lu, Y. D. Yin, *Langmuir* **2011**, *27*, 5282.
[9] B. D. Smith, N. Dave, P. J. J. Huang, J. W. Liu, *J. Phys. Chem. C* **2011**, *115*, 7851.
[10] S. Lin, M. Li, E. Dujardin, C. Girard, S. Mann, *Adv. Mater.* **2005**, *17*, 2553.
[11] R. Wilson, *Chem. Soc. Rev.* **2008**, *37*, 2028.
[12] D. A. Giljohann, D. S. Seferos, W. L. Daniel, M. D. Massich, P. C. Patel, C. A. Mirkin, *Angew. Chem.* **2010**, *122*, 3352; *Angew. Chem., Int. Ed.* **2010**, *49*, 3280.
[13] Z. X. Wang, L. N. Ma, *Coord. Chem. Rev.* **2009**, *253*, 1607.
[14] Z. S. Wu, H. X. Lu, X. P. Liu, R. Hu, H. Zhou, G. L. Shen, R. Q. Yu, *Anal. Chem.* **2010**, *82*, 3890.
[15] B. A. Kong, A. W. Zhu, Y. P. Luo, Y. Tian, Y. Y. Yu, G. Y. Shi, *Angew. Chem.* **2011**, *123*, 1877; *Angew. Chem., Int. Ed.* **2011**, *50*, 1837.
[16] C. Guarise, L. Pasquato, V. De Filippis, P. Scrimin, *PNAS* **2006**, *103*, 3978.
[17] W. Zhao, M. A. Brook, Y. F. Li, *ChemBioChem* **2008**, *9*, 2363.
[18] Y. W. Lin, C. C. Huang, H. T. Chang, *Analyst* **2011**, *136*, 863.
[19] M. R. Knecht, M. Sethi, *Anal. Bioanal. Chem.* **2009**, *394*, 33.
[20] Y. L. Hung, T. M. Hsiung, Y. Y. Chen, C. C. Huang, *Talanta* **2010**, *82*, 516.
[21] L. H. Wang, J. Li, S. P. Song, D. Li, C. H. Fan, *J. Phys. D: Appl. Phys.* **2009**, *42*, 203001.
[22] H. Lee, T. Kang, K. A. Yoon, S. Y. Lee, S. W. Joo, K. Lee, *Biosens. Bioelectron.* **2010**, *25*, 1669.
[23] J. K. Wu, L. Y. Li, D. Zhu, P. A. He, Y. Z. Fang, G. F. Cheng, *Anal. Chim. Acta* **2011**, *694*, 115.
[24] C. W. Liu, Y. T. Hsieh, C. C. Huang, Z. H. Lin, H. T. Chang, *Chem. Commun.* **2008**, 2242.
[25] C. J. Yu, T. L. Cheng, W. L. Tseng, *Biosens. Bioelectron.* **2009**, *25*, 204.
[26] B. L. Li, Y. Du, S. J. Dong, *Anal. Chim. Acta* **2009**, *644*, 78.
[27] G. K. Darbha, A. K. Singh, U. S. Rai, E. Yu, H. T. Yu, P. C. Ray, *J. Am. Chem. Soc.* **2008**, *130*, 8038.
[28] C. C. Huang, H. T. Chang, *Chem. Commun.* **2007**, 1215.
[29] H. B. Li, Q. L. Zheng, C. P. Han, *Analyst* **2010**, *135*, 1360.
[30] Y. J. Kim, R. C. Johnson, J. T. Hupp, *Nano Lett.* **2001**, *1*, 165.
[31] K. Yoosaf, B. I. Ipe, C. H. Suresh, K. G. Thomas, *J. Phys. Chem. C* **2007**, *111*, 12839.
[32] Y. F. Zhang, B. X. Li, X. L. Chen, *Microchim. Acta* **2010**, *168*, 107.
[33] L. Li, B. X. Li, *Analyst* **2009**, *134*, 1361.
[34] X. Y. Wei, L. Qi, J. J. Tan, R. G. Liu, F. Y. Wang, *Anal. Chim. Acta* **2010**, *671*, 80.
[35] B. Roy, A. Saha, A. K. Nandi, *Analyst* **2011**, *136*, 67.
[36] W. J. Qi, D. Wu, J. Ling, C. Z. Huang, *Chem. Commun.* **2010**, *46*, 4893.
[37] D. A. Feng, Y. Y. Zhang, W. Shi, X. H. Li, H. M. Ma, *Chem. Commun.* **2010**, *46*, 9203.
[38] C. L. Schofield, R. A. Field, D. A. Russell, *Anal. Chem.* **2007**, *79*, 1356.
[39] Y. Zheng, Y. Wang, X. R. Yang, *Sens. Actuators, B* **2011**, *156*, 95.
[40] T. T. Lou, Z. P. Chen, Y. Q. Wang, L. X. Chen, *ACS Appl. Mater. Interfaces* **2011**, *3*, 1568.
[41] F. Tan, X. Liu, X. Quan, J. W. Chen, X. N. Li, H. X. Zhao, *Anal. Methods* **2011**, *3*, 343.
[42] J. F. Zhang, M. Park, W. X. Ren, Y. Kim, S. J. Kim, J. H. Jung, J. S. Kim, *Chem. Commun.* **2011**, *47*, 3568.
[43] S. K. Kim, D. H. Lee, J. I. Hong, J. Yoon, *Acc. Chem. Res.* **2009**, *42*, 23.
[44] X. M. Huang, Z. Q. Guo, W. H. Zhu, Y. S. Xie, H. Tian, *Chem. Commun.* **2008**, 5143.
[45] M. Ronaghi, S. Karamohamed, B. Pettersson, M. Uhlen, P. Nyren, *Anal. Biochem.* **1996**, *242*, 84.
[46] S. Xu, M. He, H. Yu, X. Cai, X. Tan, B. Lu, B. Shu, *Anal. Biochem.* **2001**, *299*, 188.
[47] C. Y. Lin, C. J. Yu, Y. H. Lin, W. L. Tseng, *Anal. Chem.* **2010**, *82*, 6830.

Received: November 5, 2011
Published online: February 29, 2012

